11-7-2022

Missing Teeth and Restoration Detection Using Dental Panoramic Radiography Based on Transfer Learning With CNNs

Shih-Lun Chen
CYCU, Chung Yuan Christian University

Tsung-Yi Chen
CYCU, Chung Yuan Christian University

Yen-Cheng Huang
Chang Gung Memorial Hospital

Chiung-An Chen
Ming Chi University of Technology

He-Sheng Chou
CYCU, Chung Yuan Christian University

See next page for additional authors

Custom Citation

Chen, S.L., Chen, T.Y., Huang, Y.C., Chen, C.A., Chou, H.S., Huang, Y.Y., Lin, W.C., Li, T.C., Yuan, J.J., Abu, P.A.R., & Chiang, W.Y. (2022). Missing Teeth and Restoration Detection Using Dental Panoramic Radiography Based on Transfer Learning With CNNs. IEEE Access, 10, 118654-118664. https://doi.org/10.1109/ACCESS.2022.3220335

IEEE Access
Multidisciplinary | Rapid Review | Open Access Journal

Received 7 October 2022, accepted 29 October 2022, date of publication 7 November 2022, date of current version 16 November 2022.

Digital Object Identifier 10.1109/ACCESS.2022.3220335

RESEARCH ARTICLE

Missing Teeth and Restoration Detection Using Dental Panoramic Radiography Based on Transfer Learning With CNNs

SHIH-LUN CHEN[1], (Member, IEEE), TSUNG-YI CHEN[1], YEN-CHENG HUANG[2], CHIUNG-AN CHEN[1,3], HE-SHENG CHOU[1], YA-YUN HUANG[1], WEI-CHI LIN[1], TZU-CHIEN LI[1], JIA-JUN YUAN[1], PATRICIA ANGELA R. ABU[4], (Member, IEEE), AND WEI-YUAN CHIANG[3,5]

[1]Department of Electronic Engineering, Chung Yuan Christian University, Chung-Li 32023, Taiwan
[2]Department of General Dentistry, Chang Gung Memorial Hospital, Taoyuan 33305, Taiwan
[3]Department of Electronic Engineering, Ming Chi University of Technology, New Taipei 24301, Taiwan
[4]Department of Information Systems and Computer Science, Ateneo de Manila University, Quezon 1108, Philippines
[5]National Synchrotron Radiation Research Center, Hsinchu 30076, Taiwan

Corresponding author: Chiung-An Chen (joannechen@mail.mcut.edu.tw)

This work was supported in part by the Ministry of Science and Technology, Taiwan, under Grant MOST MOST-111-2221-E-033-041, Grant 111-2823-8-033-001, Grant 111-2622-E-131-001, Grant 110-2223-8-033-002, Grant 110-2221-E-027-044-MY3, Grant 110-2218-E-035-007, Grant 110-2622-E-131-002, Grant 109-2622-E-131-001-CC3, Grant 109-2221-E-131-025, and Grant 109-2410-H-197-002-MY3; and in part by the National Chip Implementation Center, Taiwan.

ABSTRACT Common dental diseases include caries, periodontitis, missing teeth and restorations. Dentists still use manual methods to judge and label lesions which is very time-consuming and highly repetitive. This research proposal uses artificial intelligence combined with image judgment technology for an improved efficiency on the process. In terms of cropping technology in images, the proposed study uses histogram equalization combined with flat-field correction for pixel value assignment. The details of the bone structure improves the resolution of the high-noise coverage. Thus, using the polynomial function connects all the interstitial strands by the strips to form a smooth curve. The curve solves the problem where the original cropping technology could not recognize a single tooth in some images. The accuracy has been improved by around 4% through the proposed cropping technique. For the convolutional neural network (CNN) technology, the lesion area analysis model is trained to judge the restoration and missing teeth of the clinical panorama (PANO) to achieve the purpose of developing an automatic diagnosis as a precision medical technology. In the current 3 commonly used neural networks namely AlexNet, GoogLeNet, and SqueezeNet, the experimental results show that the accuracy of the proposed GoogLeNet model for restoration and SqueezeNet model for missing teeth reached 97.10% and 99.90%, respectively. This research has passed the Research Institution Review Board (IRB) with application number 202002030B0.

INDEX TERMS Biomedical image, panoramic image, histogram equalization, flat-field correction, tooth segmentation, tooth position, CNN, transfer learning, Alexnet, GoogLeNet, Squeezenet.

I. INTRODUCTION

In the past two decades, with the development of science and technology, R&D personnel have cooperated with physicians of various disciplines to research a large of patient data through comprehensive applications and carry out more innovative procedures. By processing patient data and data from comprehensive studies around the world, deep learning has made significant developments in the medical field, such as X-ray [1], MRI [2], gastroscopy [3], and other medical projects related to imaging. It also has significant help in the diagnosis of medical imaging symptoms, for example, cell

The associate editor coordinating the review of this manuscript and approving it for publication was Yongjie Li.

classification [4], tumor lesions [5], and vascular analysis [6]. In proteomic analysis, by integrating proteomic information and combining structural deep network embedding (SDNE) framework [7]. From large-scale disease genomes to integration to disease genome analysis and revealing the genetic basis. CNN can automatically learn the different characteristics of each disease symptom and analyze the importance of the characteristics and the correlation between the symptoms, and then get the best function solution.

Panoramic (PANO) X-ray film is one of the dental X-rays commonly used in daily dental examinations. Compared to other dental X-ray films, it has the important advantage of covering most anatomical structures and clinical findings in a single image [8]. This important feature facilitates analysis by PANO experts and provides important information related to clinical diagnosis and treatment [9]. In this study, deep learning will be used to classify different symptoms of teeth. Regarding deep learning in the development of dental symptoms, more analysis of the risks and potential results of certain procedures can be carried out. This also helps dentists to show patients about correcting teeth [10], if they receive a complete smile overhaul in the form of a complete arch implant and restoration, what effect they will see. This is a considerable revolution in dentistry, and it hasn't even stopped there. In [11], focus on the system for detecting and segmenting each tooth in panoramic X-ray images. In [12], for the realization of a 2-level hierarchical CNN structure for tooth segmentation by labeling each mesh surface: for the gums Marking and use for interdental marking. The work proposing a novel approach based on the sparse voxel octree and 3D convolution neural networks (CNNs) for segmenting and classifying tooth types on the 3D dental models in [13]. Most of the researches only go to the segmentation of teeth and does not use these segmented images for further training. Therefore, this topic will use these Complete the cut pictures to continue the model training on dental symptoms. In this study, the previous research results [14] will be used to separate the teeth into a single sample for the tooth cutting of the X-ray ring dental film. And to perform tooth identification beyond wisdom teeth with through-like changes and spatial relationships Technology [15], and the recent automatic identification of tooth position based on Mask-RCNN [16] to discuss the accuracy. In this study, the technology of cutting teeth will be improved to increase accuracy. At the same time, according to the different feature values of the judged symptoms, image enhancement will be used to enhance the features of each disease. The transfer training of deep learning, the establishment of artificial intelligence models of related symptoms, to judge the symptoms.

Among the many dental diseases, this study focuses on the analysis and discussion of missing teeth and restoration, because the two types of symptoms are very common. Before performing deep learning training, the images need to be enhanced with symptoms. This study mainly uses the difference in pixel values of the two symptoms to distinguish them and to judge the symptoms. The first is contrast adjustment [17]. First, contrast adjustment is used to amplify the characteristics of pixel values, and then median filtering [18] is used to eliminate noise on the image after contrast adjustment. This process is model training. The symptoms of the previous image are strengthened. At the same time, for the non-target part, the background masking technology is used to cover the background of the cut teeth, so that the model during training can better train the characteristics of the disease so that the sample of the tooth cut complete picture is more Become complete. After the enhancement processing of the image symptoms is completed, the model will be trained. Here, three models of transfer training are used, namely AlexNet, GoogLeNet, and SqueezeNet [19] adjust its hyperparameters and learning rate to improve the accuracy of the model when training this symptom, perform symptom training for various image processing, and compare the correctness rate to find the most suitable CNN model training. Then use the most suitable CNN model of the two symptoms to integrate, and get the most suitable system structure. Each model contains different amounts of layers and nodes, producing the different classification methodology. The novelties of the proposed method are as follows:

1. The research uses histogram equalization combined with the flat-field correction to assign pixel values. It depicts the bone structure more clearly, and also improves the resolution of high-noise coverage.

2. The research uses the polynomial function to connect all the interstitial strands by the strips to form a smooth curve. It solves the problem that the original cutting technology could not take out a single tooth in some images in the [14].

3. This proposal uses image preprocessing technology and masking technology to increase the final accuracy by up to 5.4% (from 91.7% to 97.1%).

4. From the results, the accuracy rates of the five models are all above 95%. Among them, the accuracy rate of GoogLeNet reached 97.1%. Compared with the reference, the accuracy rate is improved by about 7%.

The analysis method of missing teeth and restoration in dental panoramic proposed in this research can provide dentists with more accurate objective judgment data, so as to achieve the purpose of developing automatic diagnosis and treatment plans as a technology for assisting precision medicine. The proposed method not only reduces the workload of dentists, but also allows them to have more time for professional clinical treatment, improves the quality of medical resources, and achieves the goal of a harmonious doctor-patient relationship.

The introduction structure of this research is followed by the introduction of materials and methods for the analysis model of missing teeth and restoration based on the convolutional neural network (CNN). The third part introduces and analyzes the evaluation methods and experimental results of the model. Then, these findings are discussed in Section 4. Finally, the fifth section puts forward conclusions and future prospects.

II. IMAGE CROPPING AND POSITIONING PREPROCESSING ALGORITHM

In the past 10 years, there have been more and more cutting methods for Dental Panoramic Radiograph (DPR), whether in traditional image extraction algorithms or automatic cutting based on neural network architecture, such as using threshold adjustment to extract feature segmentation [20], or use edge detection to generate clearer images, and improve the success rate of techniques such as segmentation of objects and feature extraction from the image [21]. Computer vision networks also have different performances in medical treatment and have achieved outstanding results in judging dental diseases. In this research, this paper improved the past cutting algorithm [14], and performed symptom enhancement imaging technology before performing CNN training and verification, and used different CNN architectures such as the current common networks, AlexNet, GoogLeNet, and SqueezeNet. Performs migration learning on the above network and is used to determine whether a single tooth after cutting has missing teeth or restoration. Finally, the above three network architectures are integrated, and each network is used to identify the correct rate of different symptoms and select the architecture to adapt to this disease.

The overall flow chart of this study is presented in Figure. 1. First, a single tooth segmentation algorithm is performed on the input image. The detailed steps of this part will be described in detail in Section 2.1. Next, the clinical imaging database is built. The database requires samples with different symptoms with the same number of images. Therefore, the number of samples must be balanced. After the database is established, it needs to be divided into two, one for the training set and another for the verification set. This article uses a common ratio conFigureuration of 7:3 and uses random classification so that the model can get a better learning effect. Finally, the actual symptoms are judged to confirm the performance of the model. A large number of samples is necessary for training a good CNN network. To obtain better results, data enhancement technology will be carried out before training that includes horizontal mirroring, vertical inversion, etc., to expand the existing number of training data several times allowing the model to acquire and learn more features of the disease. The data volume enhancement technology only uses the augmentation of the data volume during training.

A. SEGMENTED TOOTH IMAGE

In the research of authors such as VE Rushton, K Horner, and HV Worthington, it is found that dentists usually take a dental panoramic radiograph (DPR) for planning oral surgery, facial trauma, periodontal disease, heavily restored dentition, and patient first attendance. DPR acquisition is mainly used as a general screen and to view unerupted or impacted teeth. Opinions of dentists on the diagnostic usefulness of DPR are broadly consistent with those in the scientific literature [22]. However, a DPR includes many details including the full-mouth teeth, tooth root development, mandibular joints, sinuses, and maxillary sinuses. If DPR images are used directly for diagnosis it might lead to inaccuracies since the amount of image information is too rich therefore leading to wrong judgments. With that, the image processing technology of extracting a single tooth image must be performed first. The main step is to separate the images of the upper and lower rows of teeth and then divide the photos into individual teeth thus the center of gravity of the judgment can be changed from the original whole picture to that of the current tooth. Moreover, this can make it convenient to build a database of training and testing for the Database setting.

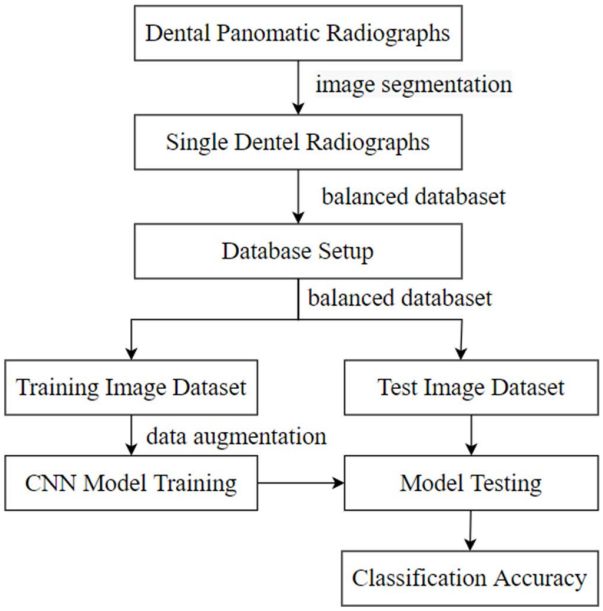

FIGURE 1. Flow chart of the entire method.

1) IMAGE PREPROCESSING

There are no segmentation methods developed precisely for panoramic X-rays. One of the challenges of developing one is that the variations between the individual tooth are not apparent. In this study, enhancing the contrast of the image between the region of interest and the background can carry out a better approach to the segmentation process.

In the proposed segmentation method in this study, it first enforces an edge sharpening to the contours of each tooth which isolates the pixel boundary between the tooth and the occlusion cavity as illustrated in Figure. 2(a). Second step involves the use of histogram equalization to distribute the pixel values, not only depicting the bone structure more sharply but also improving the feature point of the teeth, therefore, bringing the CNN training results at a higher rate of identification accuracy as shown in Figure. 2(b). After performing square equilibrium, and flat-field correction approval the resolution is covered by advanced noise as illustrated in Figure. 2(c). Finally, the adaptive histogram equalization approach balanced the contrast of the image to identify more regions of interest as shown in Figure. 2(d). All of the above-mentioned image processing steps are utilized to

obtain more detail from the teeth. Maintaining a stronger contrast between teeth and gaps showed a significant improvement in the segmentation compared with directly using the original image.

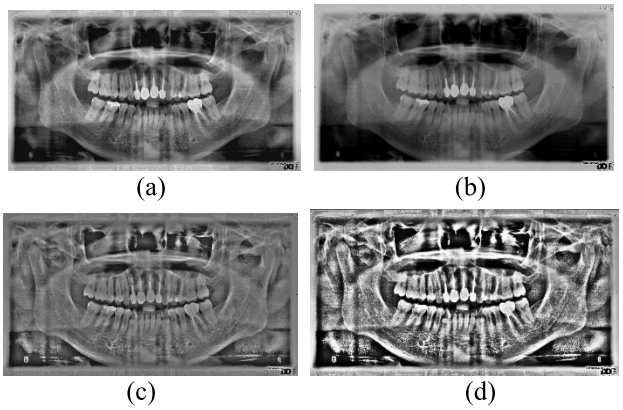

FIGURE 2. Image preprocessing process (a) Sharpening; (b) Contrast segmentation; (c) Flat-field correction; (d) Adaptive histogram equalization.

2) IMPROVED UPPER JAW AND LOWER JAW SEGMENTATION

The method presented in [23] for separating the upper and lower jaws uses horizontal integral projection to detect the gap between the teeth to segment the oral image into equal straight slices. Due to the location of the gap which should have a higher total amount of the pixel value than the location part of the tooth, several discontinuous horizontal lines are found to divide the adjacent teeth. After the points have been found for the whole image, a spline function is used to form a smooth line separating the upper and lower jaws. This method requires a probability calculation by having the user to manually enter the possible position of the gap valley making this step and segmentation part a semi-automatic segmentation.

To achieve the purpose of performing an automated processing, the center point is automatically delineated within the range of 55% to 60% relative to the vertical height of the image. This range is chosen because it is usually the position where the patient bites the locator when taking panoramic X-rays. Furthermore, from the improvements from reference [14], users need to manually input the center point technology. Then the image is horizontally cut into several equal parts. After the experiments, it is found that the more cuts there is, the more accurate is the identified curve. However, if the number of divisions is way too much, unnecessary noise is likely to appear on the image. Therefore, the appropriate number of divisions must be set to make the curve of the divided oral cavity more accurate. Finally, an algorithm similar to horizontal integration is applied which determines the position of the center vertical of the gap valley. Relative to this point, a 5% range boundary to the area of the next vertical feature point calculation is set. This approach is constantly applied looking for both sides of each and every tooth. After identifying all the vertical segment lines based on the center part of each line as a mark, the curve line is drawn by applying the polynomial function therefore resulting to a marked imaged as shown in Figure. 3.

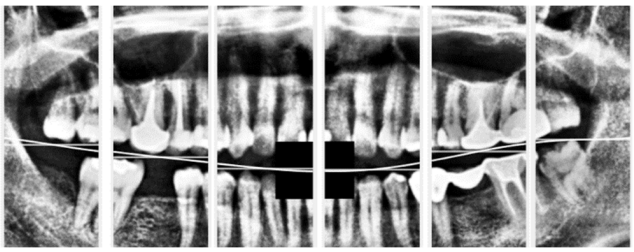

FIGURE 3. After substituting the polynomial function, the smooth curve is obtained.

3) IDENTIFY TEETH GAPS

The neck of the teeth is a blurred line between the crown and the gums of teeth as illustrated in Figure. 4. It is located next to the tooth gap, sitting in the middle of the tooth. In the dental neck, there is a pulp cavity structure that contains blood vessels and nerves. Its density is relatively low compared to the white franc and dentin. In clinical images, its pixel value under X-ray irradiation is significantly lower than the white franc and dentin.

According to the above characteristics, step 2.1.2 can be used to find a curve that passes through the tooth gap and the tooth neck. Parallel shifting up and down, thus comparing the sum of the pixels on each translation curve, the sum of the smallest pixel count is the target position. This method is similar to the integral projection method. To avoid over-detection problems, 5 pixels is added to the curve line thus making it wider, and automatically deleting the distance range that is located too close and too far. It is roughly equivalent to the distance separating the upper and lower jaw curves, ranging from one-third to two-thirds of the teeth. Through this step, one upper dental suture line and one lower dental suture line can be obtained as shown in Figure. 4.

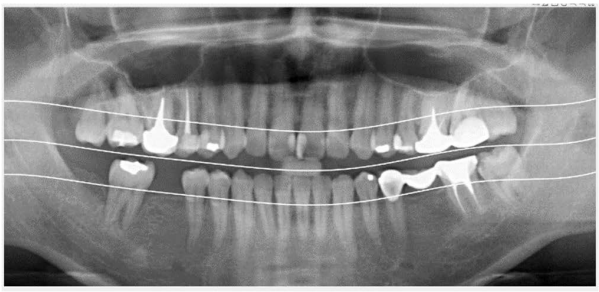

FIGURE 4. Schematic diagram of the location of the identified upper and lower dental sutures.

After identifying the interdental gap, the interdental point on this curve is identified as well. Ideally, the location of the tooth seam pixel value will be relatively low. Reference [24] proposes to use the average width of the tooth to search for iteratively. It is then defined as the interdental point to find 8 interdental points. That completes the searching of one

side. Apparently, this method is more complicated. Therefore, this article proposes an alternatively simple way to improve the method of finding the interdental points proposed in reference [24].

The previously identified interdental line is used to find the local minimum value instead of searching the entire image. This step can be used for preliminary screening of interdental points as illustrated in Figure. 5(a). The missing points are mainly caused by overlapping or missing teeth. Due to the different sizes of teeth, the width between molars, canines, and incisors varies. Using this feature, teeth can be roughly divided into these three categories and are judged by different positions. The distance between the interdental points and the location of the interdental points can be used to fill the areas where the interdental gaps are lost due to overlapping or continuous missing teeth as shown in Figure. 5(b).

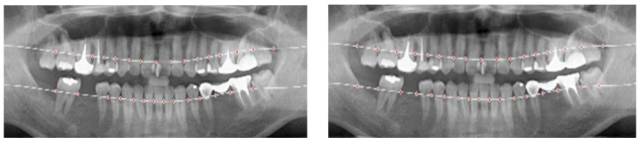

FIGURE 5. Position of the interdental point obtained by the proposed method in this article. (a) Position of the interdental point after the preliminary screening. (b) Image after the filling point.

4) TEETH SEGMENTATION

When drawing the cutting lines, different methods of cutting are implemented taking into account the different characteristics of the upper and lower rows of teeth photographs. Greedy Algorithm [25] is a fast iterative approach that always selects the optimal solution in the current situation when solving a problem. However, it does not take into account the overall performance which in other words, is the local optimal solution. This method can be used to effectively cut the upper teeth.

According to the Greedy Algorithm Rule concept, the method will move 1 pixel up each iteration from the tooth seam point and look for the lowest value between the five pixels horizontally. It uses this point as the starting point for the next iteration, repeating until half the length of the tooth, and then connecting the position to the corresponding tooth seam point into a split line as shown in Figure. 6. This method is utilized for the upper part of the cut. Compared to the lower half of the teeth, the upper part of the teeth is generally large and scattered. There will be no lower front teeth that is too small where the edges are not clear problems.

In separating teeth, the pixel strength is summed up by using each line perpendicular to the curve [26]. Because the gap between adjacent teeth causes the value projected on the curve to be very low, the teeth can be split in this way. Although this is a great method, in practice, teeth will have overlap problems that are not necessarily the so-called gaps especially in the lower half. This is mainly because the lower front teeth are too small to overlap thus teeth that will appear or lead to similar to the above is not applicable. With that, this

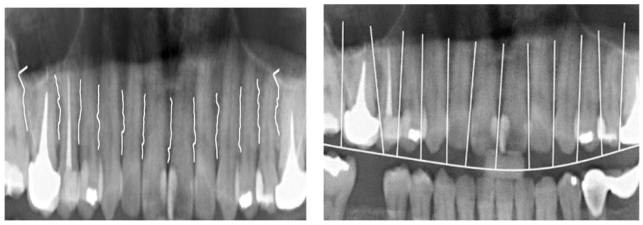

FIGURE 6. The method of cutting the upper half of the teeth. (a) Starting from the interdental point, using the Greedy Algorithm to recursively find the cutting point close to the root of the tooth. (b) Drawing the cutting line using the cutting point and the interdental point that intersects on the oral cavity curve.

article also considers this case and improves on this. Inverting the method in [26], the tangent perpendicular to the curve can be obtained in reverse when the curve and the gap point are available, and the tangent is used to cut the tooth as shown in Figure. 7.

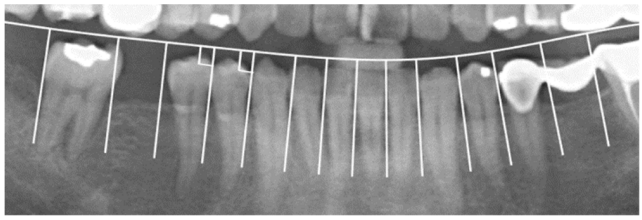

FIGURE 7. Schematic diagram of the method of cutting the lower teeth vertically.

B. DATA SET

Training CNN requires the preparation of a large number of tagged data sets to ensure the accuracy of the CNN model. Therefore, this study collaborated with three professional dentists. The clinical images were annotated by dentists. All experts are employed in specialist clinics and have at least 3 years of clinical experience. Experts guide researchers, provide symptom knowledge, teach researchers with actual cases (describe the characteristics of missing teeth and restoration), and provide clinical data to calibrate the CNN model (eliminate other non-target symptoms).

To reduce the computational complexity of the developed algorithm, this study used a single tooth to judge the results. The image library annotated by the dentists was also based on the single tooth for marking as described in step 2.2. A total of 108 panoramic X-rays were used to obtain a total of 3,456 dental images of the single tooth. With the help of a dentist, each tooth has been marked with signs of disease.

Since the data were provided by the hospital, there isa significant imbalance in the proportion of image with only 498 dentures and 358 missing teeth, compared with 2,600 normal teeth. Table 1 shows the number of images for each clinical disease type, with the number of normal teeth far higher than the remaining two diseases. To train on limited data and avoid having CNN models that are under-represented by insufficient data, data enhancement

techniques were applied that include random rotation, random scaling, vertical, and horizontal flipping to expand the database. The expanded images are automatically generated and used for training and are not used in verifying CNN models to prevent confusion.

TABLE 1. The distribution of the symptoms in this research database.

	Quantity of Findings			
	Restoration	Missing	Normal	Total
Quantity	498	358	2600	3456

After the image is trimmed, the size of the image is not uniform. If the size of the image is not uniformly specified, it cannot be put into CNN for training and judgment. Therefore, the images in the database must be standardized, so that the pixels of each tooth image are fixed to $227 \times 227 \times 3$. But such behavior will force the image to be compressed to a fixed size, changing the original image shape features that can be used as a basis for judgment.

To strengthen the recognition effect of CNN, the reference paper in [27] proposed a method to enhance the contrast of the original cut teeth which can highlight the abnormal condition of the teeth. In addition, the masking technology for the tooth and the tangent obtained in step 2.1.4. are used to cover the part that does not belong to the tooth, and let the CNN remove the non-objective part. The result of the image processing steps is shown in Figure. 8. However, these steps are not guaranteed to be helpful for training. To prove that these methods are effective, the help of different processing for training the network is compared in step C.

C. NEURAL NETWORK

Neural networks (NNs) are also known as artificial neural networks (ANN). By simulating the way neurons in the human brain operate in the nervous system, we can deal with complex mathematical problems, analyze and judge. Deep learning is a new technique of image classification. CNN is one of those deep learning networks that train it with tagged training sets.

1) TRANSFER LEARNING

Transfer learning is to use a network that has been designed and trained to fine-tune it to make these networks fit in different situations. Considering that most data and different fields have their correlation, the trained model can be used to help the training of the new model through transfer learning. It is a very difficult task to rebuild a complete network. Even if a network is built, there is still a long way to go in the accuracy of learning and parameter setting. The use of the built model can ensure the operation completeness and accuracy of results which can greatly reduce development time.

In this study, AlexNet, GoogLeNet, and SqueezeNet are used. These three models are all constructed and trained

FIGURE 8. Image processing of a single tooth image. (a) Original image without judgment preprocessing; (b) Contrast-enhanced image processing result; and (c) The image after covering other teeth.

networks. Alexnet, currently a widely used model, uses a stochastic gradient descent algorithm to find the best results that is based on an iterative algorithm to find the smallest value of the loss function [28]. GoogLeNet on the other hand began to emerge in 2014 through a complex network with a higher accuracy [29]. Especially for complex networks, it uses a skillful way to overcome the problems encountered by increasing the nerves of the network. SqueezeNet is a very small network [30] whose purpose is to reduce the number of parameters, increase the speed, and reach the accuracy of AlexNet. Its parameters are nearly 50 times less than that of AlexNet.

2) HYPERPARAMETER ADJUSTMENT

Hyperparameter settings account for a very important factor in the training of a model. A good model requires many attempts to find a suitable setting. The hyperparameter settings in this study are listed in Table 2. In terms of settings, the three training models all use the same parameters for training. This study uses a fixed LearningRate instead of changing the LearningRate for different Epochs.

(a) MiniBatchSize: The minimum amount of data used for each iteration of training.
(b) MaxEpoch: An Epoch means that all samples in the training set have been trained once.
(c) LearningRate: The learning rate determines the neural network and aims to achieve higher accuracy. Usually the smaller the value is, the more accurate the result will

be. But if it is too small, it is easy to overfit the neural network.

(d) ValidationFrequency: After multiple BatchSize, a validation is performed.

TABLE 2. Hyperparameter settings in this study.

Minibatchsize	Maxepochs	Learning Rate	Validation Frequency
16	12	0.0001	5

In addition to the above hyperparameters, this study uses the gradient descent algorithm as the optimization function. After each training and verification, the gradient of the loss function is calculated and the internal weights are updated. For ValidationPatience, no conditions are set but the overall training is executed to a MaxEpoch of 12 times. The network to avoid training just meets the conditions but the actual training has not yet been completed. Finally, the Shuffle method is used for each Epoch which allows images to enter the network in an irregular form for training rather than in a fixed order.

3) TRAINING PHASE

In 2.2. Data Setup, the problem of unevenness and lack of data was mentioned. To train on limited data, the CNN model is avoided from affecting the learning effect due to insufficient and uneven data.

This study randomly selects 350 images for each disease symptom from the database where 70% is used as the training set and the remaining 30% is used as the verification set. The training set is the set of samples needed to train a network, and the validation set is the set of samples used to evaluate whether the network can distinguish correctly after training. Data enhancement techniques are applied to the training set. These techniques include random angle rotation of $\pm 20°$, random zoom, vertical and horizontal flips, and vertical and horizontal translation of ± 30 pixels to increase training image set complexity and number of samples. Through this method, the training set can generate 5145 tooth images and each judgment sample has 1715 images for training.

III. EXPERIMENTAL RESULTS AND ANALYSIS

This chapter will present the performance results of the proposed tooth segmentation algorithm and compare it with the proposed method in reference [14]. A comparison on the effect of the image processing of the data set with the results of the three CNN networks will be presented for further results discussion.

A. THE PERFORMANCE OF THE TOOTH CUTTING ALGORITHM

From the 108 Dental Panoramic Radiographs in the original data set, the improved cutting method is used to accurately segment each tooth. Table 3 lists the accuracy of cutting and positioning of the cutting method proposed in this article on all 32 teeth. The marking method of the teeth is illustrated in Figure. 9. It can be seen that in tooth positions 15, 14, 13, 21, 22, 27, 34, 32, and 42, the accuracy rate exceeds 95%. In teeth 12, 11, 33, 31, and 41, it is even more than 98%. The overall accuracy rate is 93.28%. This shows the excellent performance of tooth cutting and tooth positioning presented in this article. Compared with the 92.78% and 92.14% accuracy rates in [14] and [15], the accuracy rate in this study showed a 0.5% improvement as listed in Table 4. Even compared with 79.00% of the literature [13], the proposed method is a huge improvement.

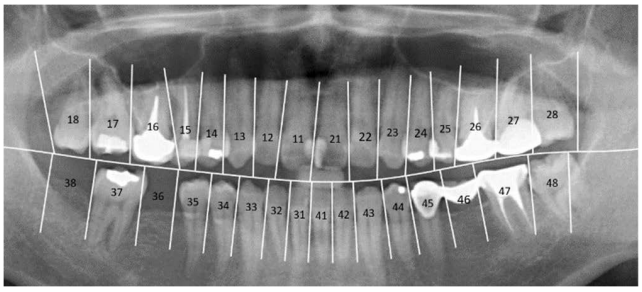

FIGURE 9. Schematic diagram of the numbering method of international teeth.

TABLE 3. Accuracy of cutting on different tooth positions.

Number	Accuracy (%)	Number	Accuracy (%)
11	99.11	31	98.21
12	98.21	32	96.43
13	97.32	33	98.21
14	96.43	34	95.54
15	95.54	35	94.64
16	94.64	36	92.86
17	92.86	37	91.96
18	92.86	38	91.96
21	97.32	41	99.11
22	96.43	42	97.32
23	93.75	43	92.86
24	91.07	44	91.07
25	87.50	45	87.50
26	85.71	46	86.61
27	96.61	47	84.82
28	87.50	48	83.04

TABLE 4. Positioning accuracy rate.

Number	**This Study**	Huang et al. [14]	Park et al. [15]	Wirtz et al. [16]
Positioning Accuracy Rate	**93.28%**	92.78%	92.14%	79.00%

B. COMPARISON OF DIFFERENT CNN NETWORKS

Through the status of CNN training, it can be judged whether the effect of image processing is useful. This article uses three

kinds of networks (AlexNet, GoogLeNet, and SqueezeNet) to train the four kinds of data, and finally judge their performance in terms of accuracy specifically on the following: no cover and no pretreatment (original image), no cover and pretreatment, cover and no pretreatment, and cover and pretreatment as listed in Table 5.

TABLE 5. Accuracy of the three models.

	AlexNet	GoogleNet	SqueezeNet
Original mage	90.5%	91.7%	92.4%
Pretreatment	94.9%	94.0%	96.2%
Masking	94.3%	95.9%	96.2%
Pretreatment & masking	95.2%	97.1%	95.2%

In the case of preprocessing or masking, there is a significant improvement in the accuracy of all networks. Compared with the original image, the accuracy rate was 94% and the highest was 96.2%. The difference from the original image was up by about 4.2%. This indicates that pre-training is effective. However, with preprocessing and masking performed together, the SqueezeNet was not as good as expected with a significant decrease in accuracy, while AlexNet and GoogLeNet showed a significant increase.

The accuracy and loss function evaluation of the training process of these three models are shown in Figure 10 and Figure 11, respectively. In order to evaluate the performance and accuracy of different CNN models, the indicators of precision and recall [31], [32], and [33] are used. These indicators are widely used to evaluate the modulus. The calculation formulas of precision, recall, and accuracy are shown in equations (1)∼(3):

$$Accuracy = \frac{TP + TN}{TP + FP + TN + FN} \tag{1}$$

$$Precision = \frac{TP}{TP + FP} \tag{2}$$

$$Recall = \frac{TP}{TP + FN} \tag{3}$$

TP is a true positive, FP is a false positive, TN is a true negative, and FN is a false negative.

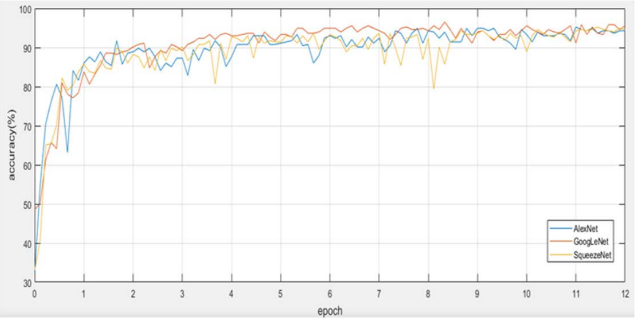

FIGURE 10. The accuracy of the training process of the three models.

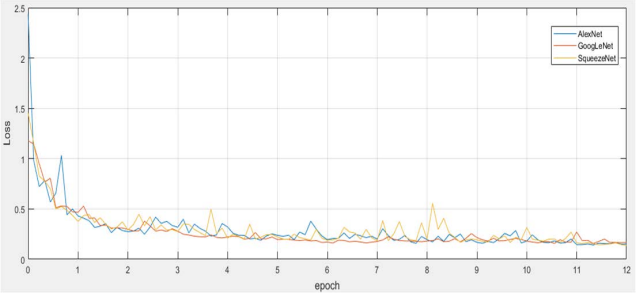

FIGURE 11. Loss function evaluation for the training process of the three models.

TABLE 6. Precision and recall of the three models using the images for feature enhancement.

Type		Missing	Normal	Restoration
AlexNet	Precision	93.30%	99.00%	92.40%
	Recall	99.00%	89.70%	97.00%
GoogLeNet	Precision	91.40%	98.10%	92.40%
	Recall	96.00%	88.80%	98.00%
SqueezeNet	Precision	96.20%	95.20%	97.10%
	Recall	98.10%	97.10%	93.60%

After applying the different processes to the images, Tables 6, 7, and 8 above are obtained by training and testing the images as models. Higher values for precision and recall correspond to higher accuracy in detecting the disease. However in reality. different models differ in precision and recall for different diseases. For patients, there is a preference for misjudgment rather than missed detection. Under these conditions, precision is a little more important to consider than the recall.

In Table 6, after enhancing the contrast of the tooth image, the precision and recall values of the model judgment were obtained. It can be seen that SqueezeNet stands out from the other two network models. In detecting restoration, the model has the highest accuracy rate of 97.1%. This also conforms to the above mentioned values, which are acceptable for precision to be slightly lower than the recall value. As shown in Table 7, SqueezeNet detects the missing class much higher than the other two models under the masking process which can be seen from precision values of up to 99%. This indicates that SqueezeNet, with only masking, was able to find images with symptoms of tooth deficiency with 97.1% accuracy of which 2.7% were judged to be in other parts. Only 1% of the images which were judged to be missing by SqueezeNet were error detection whilethe rest were assumed to be missing teeth.

GoogleNet performs much better in Table 5 than the other models which stands with a higher accuracy rate in both

TABLE 7. Precision and recall of the three models using the masked images.

Type		Missing	Normal	Restoration
AlexNet	Precision	90.50%	100%	92.40%
	Recall	99.00%	86.10%	100%
GoogLeNet	Precision	94.30%	98.10%	92.80%
	Recall	96.10%	92.00%	100%
SqueezeNet	Precision	97.10%	98.10%	93.30%
	Recall	99.00%	94.50%	95.10%

TABLE 8. Precision and recall of the three models using the feature to enhance and masked images.

Type		Missing	Normal	Restoration
AlexNet	Precision	99.00%	92.40%	94.30%
	Recall	92.90%	96.00%	97.10%
GoogLeNet	Precision	98.10%	99.00%	94.30%
	Recall	97.20%	95.40%	99.00%
SqueezeNet	Precision	99.00%	98.10%	88.60%
	Recall	92.90%	93.60%	100%

precision and recall. This result is listed in Table 8, where as expected, GoogleNet values are higher in the same condition. In the Missing judgment, AlexNet and SqueezeNet both have precision values of 99% while the recall is only at 92.9%. The precision of GoogleNet 98.1% while the recall is 97.2%. While the sacrifice of a small number of recall values mentioned earlier is permissible, it is in cases where there is a clear gap between precision and recall values. GoogleNet, by contrast, is in overall doing well indicating that GoogleNet is still shown to have better detection of Missing. The accuracy for Restoration is even more pronounced that showed GoogleNet with better scores.

Table 9 summarizes the best results of the different models used in this study and compares them with current state-of-the-art [33], [34], and [15]. From the results, whether it is for missing teeth or Restoration, this study has better recognition accuracy. GoogleNet has the best accuracy performance in this article having an accuracy rate of 97.1%. AlexNet has 95.2% which is relatively low. The overall accuracy of the method in this paper is above 95%, which is greatly improved compared with the methods in the current state-of-the-art [33], [34], and [15].

The accuracy of tooth cutting and positioning will have a large degree of positive correlation with subsequent judgments. When the cutting and positioning are improved, the target tooth is less interfered with by non-target objects. As such the accuracy of judgment can be improved. The amount of data will also affect the quality of the model training. This study classified Restoration and Missing teeth in terms of symptoms, but dentistry has dozens of diseases and symptoms. For these undefined and trained tooth images, the accuracy of the model will decrease. The above problems will still need to be considered and overcome in the future. For practical applications in clinical use, this process can be more complete and more convenient therefore achieving the goal of an assisted precision medicine.

TABLE 9. Accuracy of the three models and compared to literature.

	This work			Lin et al. [33]	Çelik et al [34]	Park et al. [15].
	Google Net	Squeeze Net	Alex Net			
Missing teeth	**97.20%**	92.90%	92.90%	96.18%	NA	59.09%
Restoration	**99.00%**	99.90%	97.10%	84.30%	97.10% highest	NA
Accuracy	**97.10%**	96.20%	95.20%	90.24%	92.24%	59.09%

IV. CONCLUSION

This study presents an advanced image cropping method combined with CNN models for classification that are designed to solve the classification problem of Dental Panoramic Radiographs (DPR). Partial optimization on the cutting method is performed through the preprocessing of the image and is based on the characteristics of the human teeth. The optimization method takes into account the structure of the tooth, uses the neck and the interdental gap to segment, and locates the position of the tooth. This method is based on the 32 teeth samples of a normal person for cutting. The overall accuracy after tooth cutting reached 93% which is very promising.

The classification of dental diseases is performed by a neural network using transfer learning that classify the most common diseases: missing teeth and prostheses from normal teeth. The cutting method proposed in this article has some limitations. If any tooth grows in a special position, it will not be able to cut that tooth and the lack of teeth in DPR should not be too serious. The upper and lower teeth must have at least 8 teeth each. Otherwise, model will not be able to judge and execute. In [8], a collaborative model dynamically constructed is used to integrate two tooth segmentation and recognition models. This method has also been effectively proven to be more potent. In view of this, the collaborative model dynamically constructed will also be the direction of our future efforts.

Future research will focus on improving this system. The incisor part uses the most advanced R-CNN to perform tooth

numbering and incisor. Subsequent disease identification can also classify the symptoms in more detail and add other diseases and conditions to improve on the accuracy of the proposed method in this study. Finally, the whole system is to be simplified and the running time is to be shortened. Moreover, it is hoped that it can be applied to the clinical operation of dentists.

REFERENCES

[1] J. Chen, Y. Li, and J. Zhao, "X-ray of tire defects detection via modified faster R-CNN," in *Proc. 2nd Int. Conf. Saf. Produce Informatization (IICSPI)*, Nov. 2019, pp. 257–260, doi: 10.1109/IICSPI48186.2019.9095873.

[2] P. Arena, S. Baglio, L. Fortuna, and G. Manganaro, "CNN processing for NMR spectra," in *Proc. 3rd IEEE Int. Workshop Cellular Neural Netw. Appl. (CNNA)*, Dec. 1994, pp. 457–462, doi: 10.1109/CNNA.1994.381632.

[3] R. Zhu, R. Zhang, and D. Xue, "Lesion detection of endoscopy images based on convolutional neural network features," in *Proc. 8th Int. Congr. Image Signal Process. (CISP)*, Oct. 2015, pp. 372–376, doi: 10.1109/CISP.2015.7407907.

[4] M. S. Wibawa, "A comparison study between deep learning and conventional machine learning on white blood cells classification," in *Proc. Int. Conf. Orange Technol. (ICOT)*, Oct. 2018, pp. 1–6, doi: 10.1109/ICOT.2018.8705892.

[5] S. Somasundaram and R. Gobinath, "Current trends on deep learning models for brain tumor segmentation and detection—A review," in *Proc. Int. Conf. Mach. Learn., Big Data, Cloud Parallel Comput. (COMITCon)*, Feb. 2019, pp. 217–221, doi: 10.1109/COMITCon.2019.8862209.

[6] C. Kromm and K. Rohr, "Inception capsule network for retinal blood vessel segmentation and centerline extraction," in *Proc. IEEE 17th Int. Symp. Biomed. Imag. (ISBI)*, Apr. 2020, pp. 1223–1226, doi: 10.1109/ISBI45749.2020.9098538.

[7] M. Zilocchi, C. Wang, M. Babu, and J. Li, "A panoramic view of proteomics and multiomics in precision health," *iScience*, vol. 24, no. 8, Jul. 2021, Art. no. 102925, doi: 10.1016/j.isci.2021.102925.

[8] G. Chandrashekar, S. AlQarni, E. E. Bumann, and Y. Lee, "Collaborative deep learning model for tooth segmentation and identification using panoramic radiographs," *Comput. Biol. Med.*, vol. 148, Sep. 2022, Art. no. 105829, doi: 10.1016/j.compbiomed.2022.105829.

[9] T. Yeshua, "Automatic detection and classification of dental restorations in panoramic radiographs," *Issues Informing Sci. Inf. Technol.*, vol. 16, pp. 221–234, May 2019, doi: 10.28945/4306.

[10] W. Ying, T. Bao-yu, and X. Yun-ye, "The method of CAD model creation of dental shape based on 3D-CT images in orthodontics," in *Proc. Int. Conf. Adv. Technol. Design Manuf. (ATDM)*, 2010, pp. 219–221, doi: 10.1049/cp.2010.1292.

[11] G. Jader, J. Fontineli, M. Ruiz, K. Abdalla, M. Pithon, and L. Oliveira, "Deep instance segmentation of teeth in panoramic X-ray images," in *Proc. 31st SIBGRAPI Conf. Graph., Patterns Images (SIBGRAPI)*, Oct. 2018, pp. 400–407, doi: 10.1109/SIBGRAPI.2018.00058.

[12] X. Xu, C. Liu, and Y. Zheng, "3D tooth segmentation and labeling using deep convolutional neural networks," *IEEE Trans. Vis. Comput. Graphics*, vol. 25, no. 7, pp. 2336–2348, Jul. 2019, doi: 10.1109/TVCG.2018.2839685.

[13] S. Tian, N. Dai, B. Zhang, F. Yuan, Q. Yu, and X. Cheng, "Automatic classification and segmentation of teeth on 3D dental model using hierarchical deep learning networks," *IEEE Access*, vol. 7, pp. 84817–84828, 2019, doi: 10.1109/ACCESS.2019.2924262.

[14] Y.-C. Huang, C.-A. Chen, T.-Y. Chen, H.-S. Chou, W.-C. Lin, T.-C. Li, J.-J. Yuan, S.-Y. Lin, C.-W. Li, S.-L. Chen, Y.-C. Mao, P. A. R. Abu, W.-Y. Chiang, and W.-S. Lo, "Tooth position determination by automatic cutting and marking of dental panoramic X-ray film in medical image processing," *Appl. Sci.*, vol. 11, no. 24, p. 11904, Dec. 2021, doi: 10.3390/app112411904.

[15] J. Park, J. Lee, S. Moon, and K. Lee, "Deep learning based detection of missing tooth regions for dental implant planning in panoramic radiographic images," *Appl. Sci.*, vol. 12, no. 3, p. 3, Jan. 2022, doi: 10.3390/app12031595.

[16] A. Wirtz, S. G. Mirashi, and S. Wesarg, "Automatic teeth segmentation in panoramic X-ray images using a coupled shape model in combination with a neural network," in *Medical Image Computing and Computer Assisted Intervention—MICCAI*. Cham, Switzerland: Springer, 2018, pp. 712–719, doi: 10.1007/978-3-030-00937-3_81.

[17] C.-C. Huang and M.-H. Nguyen, "X-ray enhancement based on component attenuation, contrast adjustment, and image fusion," *IEEE Trans. Image Process.*, vol. 28, no. 1, pp. 127–141, Jan. 2019, doi: 10.1109/TIP.2018.2865637.

[18] C.-C. Chang, J.-Y. Hsiao, and C.-P. Hsieh, "An adaptive median filter for image denoising," in *Proc. 2nd Int. Symp. Intell. Inf. Technol. Appl.*, Dec. 2008, pp. 346–350, doi: 10.1109/IITA.2008.259.

[19] S. A. Prajapati, R. Nagaraj, and S. Mitra, "Classification of dental diseases using CNN and transfer learning," in *Proc. 5th Int. Symp. Comput. Bus. Intell. (ISCBI)*, Aug. 2017, pp. 70–74, doi: 10.1109/ISCBI.2017.8053547.

[20] A. Ajaz and D. Kathirvelu, "Dental biometrics: Computer aided human identification system using the dental panoramic radiographs," in *Proc. Int. Conf. Commun. Signal Process.*, Apr. 2013, pp. 717–721, doi: 10.1109/iccsp.2013.6577149.

[21] R. Kaur, R. S. Sandhu, A. Gera, and T. Kaur, "Edge detection in digital panoramic dental radiograph using improved morphological gradient and Matlab," in *Proc. Int. Conf. Smart Technol. Smart Nation (SmartTechCon)*, Aug. 2017, pp. 793–797, doi: 10.1109/SmartTechCon.2017.8358481.

[22] V. E. Rushton, K. Horner, and H. V. Worthington, "Factors influencing the selection of panoramic radiography in general dental practice," *J. Dentistry*, vol. 27, no. 8, pp. 565–571, Nov. 1999, doi: 10.1016/S0300-5712(99)00031-7.

[23] A. K. Jain and H. Chen, "Matching of dental X-ray images for human identification," *Pattern Recognit.*, vol. 37, no. 7, pp. 1519–1532, Jul. 2004, doi: 10.1016/j.patcog.2003.12.016.

[24] R. Wanat and D. Frejlichowski, "A problem of automatic segmentation of digital dental panoramic X-ray images for forensic human identification," in *Proc. 15th Central Eur. Seminar Comput. Graph. (CESCG)*, 2011.

[25] B. M. Patil and B. Amarapur, "Segmentation of leaf images using greedy algorithm," in *Proc. Int. Conf. Energy, Commun., Data Analytics Soft Comput. (ICECDS)*, Aug. 2017, pp. 2137–2141, doi: 10.1109/ICECDS.2017.8389830.

[26] Y.-C. Mao, T.-Y. Chen, H.-S. Chou, S.-Y. Lin, S.-Y. Liu, Y.-A. Chen, Y.-L. Liu, C.-A. Chen, Y.-C. Huang, S.-L. Chen, C.-W. Li, P. A. R. Abu, and W.-Y. Chiang, "Caries and restoration detection using bitewing film based on transfer learning with CNNs," *Sensors*, vol. 21, no. 13, p. 4613, Jul. 2021, doi: 10.3390/s21134613.

[27] A. Gurses and A. B. Oktay, "Tooth restoration and dental work detection on panoramic dental images via CNN," in *Proc. Med. Technol. Congr. (TIPTEKNO)*, Nov. 2020, pp. 1–4, doi: 10.1109/TIPTEKNO50054.2020.9299272.

[28] X. Zhang, W. Pan, and P. Xiao, "In-vivo skin capacitive image classification using AlexNet convolution neural network," in *Proc. IEEE 3rd Int. Conf. Image, Vis. Comput. (ICIVC)*, Jun. 2018, pp. 439–443, doi: 10.1109/ICIVC.2018.8492860.

[29] Z. Zhu, J. Li, L. Zhuo, and J. Zhang, "Extreme weather recognition using a novel fine-tuning strategy and optimized GoogLeNet," in *Proc. Int. Conf. Digit. Image Comput., Techn. Appl. (DICTA)*, Nov. 2017, pp. 1–7, doi: 10.1109/DICTA.2017.8227431.

[30] X. Qian, E. W. Patton, J. Swaney, Q. Xing, and T. Zeng, "Machine learning on cataracts classification using SqueezeNet," in *Proc. 4th Int. Conf. Universal Village (UV)*, Oct. 2018, pp. 1–3, doi: 10.1109/UV.2018.8642133.

[31] Y. Zhao, P. Li, C. Gao, Y. Liu, Q. Chen, F. Yang, and D. Meng, "TSAS-Net: Tooth segmentation on dental panoramic X-ray images by two-stage attention segmentation network," *Knowl.-Based Syst.*, vol. 206, Oct. 2020, Art. no. 106338, doi: 10.1016/j.knosys.2020.106338.

[32] K. Motoki, F. P. Mahdi, N. Yagi, M. Nii, and S. Kobashi, "Automatic teeth recognition method from dental panoramic images using faster R-CNN and prior knowledge model," in *Proc. Joint 11th Int. Conf. Soft Comput. Intell. Syst., 21st Int. Symp. Adv. Intell. Syst. (SCIS-ISIS)*, Dec. 2020, pp. 1–5, doi: 10.1109/SCISISIS50064.2020.9322685.

[33] N.-H. Lin, T.-L. Lin, X. Wang, W. T. Kao, H. W. Tseng, S. L. Chen, Y. S. Chiou, J. F. Villaverde, and Y. F. Kuo, "Teeth detection algorithm and teeth condition classification based on convolutional neural networks for dental panoramic radiographs," *J. Med. Imag. Health Inform.*, vol. 8, no. 3, pp. 507–515, 2018.

[34] B. Çelik and M. E. Çelik, "Automated detection of dental restorations using deep learning on panoramic radiographs," *Dentomaxillofacial Radiol.*, vol. 51, Sep. 2022, Art. no. 20220244, doi: 10.1259/dmfr.20220244.

SHIH-LUN CHEN (Member, IEEE) received the B.S., M.S., and Ph.D. degrees in electrical engineering from the National Cheng Kung University, Tainan, Taiwan, in 2002, 2004, and 2011, respectively.

He was an Assistant Professor and an Associate Professor at the Department of Electronic Engineering, Chung Yuan Christian University, Taiwan, from 2011 to 2014 and from 2014 to 2017, where he has been a Professor, since 2017. His current research interests include VLSI chip design, image processing, wireless body sensor networks, the Internet of Things, wearable devices, data compression, fuzzy logic control, bio-medical signal processing, and reconfigureurable architecture. He was a recipient of the Outstanding Teaching Award from Chung Yuan Christian University, in 2014 and 2019, respectively.

TSUNG-YI CHEN received the B.S. degree in electronic engineering from Chung Yuan Christian University, Zhongli, Taoyuan, Taiwan, in 2020, where he is currently pursuing the Ph.D. degree. His current research interests include VLSI chip design, image processing, machine learning, and bio-medical signal processing.

YEN-CHENG HUANG received the Bachelor of Dentistry degree from China Medical University, Taichung, Taiwan, in 2017. She is currently a Senior Resident with the Department of General Dentistry, Chang Gung Memorial Hospital, Taoyuan, Taiwan. Her current research interests include dental radiographic image processing and deep learning.

CHIUNG-AN CHEN received the B.S. degree in electronic engineering from Chung Yuan Christian University, Zhongli, Taoyuan, Taiwan, in 2005, and the Ph.D. degree in electrical engineering from the National Cheng Kung University, Tainan, Taiwan, in 2013. Since 2017, she has been an Assistant Professor with the Department of Electrical Engineering, Ming Chi University of Technology, Taiwan. Her current research interests include VLSI chip design, image processing, wireless body sensor networks, the Internet of Things, wearable devices, and biomedical signal and image processing.

HE-SHENG CHOU received the B.S. degree in electronic engineering from Chung Yuan Christian University, Zhongli, Taoyuan, Taiwan, in 2018, where he is currently pursuing the Ph.D. degree. His current research interests include VLSI chip design, image processing, machine learning, and bio-medical signal processing.

YA-YUN HUANG received the B.S. degree in electronic engineering from Chung Yuan Christian University, Zhongli, Taoyuan, Taiwan, in 2021, where she is currently pursuing the master's degree. Her current research interests include VLSI chip design and image processing and image compression.

WEI-CHI LIN received the degree in electronic engineering from Chung Yuan Christian University, Zhongli, Taoyuan, Taiwan, in 2018. His current research interests include VLSI chip design, image processing, and machine learning.

TZU-CHIEN LI received the degree in electronic engineering from Chung Yuan Christian University, Zhongli, Taoyuan, Taiwan, in 2018. His current research interests include VLSI chip design, image processing, and machine learning.

JIA-JUN YUAN received the degree in electronic engineering from Chung Yuan Christian University, Zhongli, Taoyuan, Taiwan, in 2018. His current research interests include VLSI chip design, image processing, and machine learning.

PATRICIA ANGELA R. ABU (Member, IEEE) received the B.S. degree in electronics and communications engineering from the Ateneo de Manila University, Philippines, in 2007, the M.S. degree in electronics engineering and microelectronics from Chung Yuan Christian University, Chung-li, Taiwan, in 2009, and the Ph.D. degree in computer science degree from the Ateneo de Manila University, in 2015. She is the Research Laboratory Head of the Ateneo Laboratory for Intelligent Visual Environment (ALIVE) and an Assistant Professor at the Department of Information Systems and Computer Science (DISCS), Ateneo de Manila University.. Her current research interests include image processing and computer vision with applications that revolve on biomedical imaging and road/transportation, anomaly detection, and the IoT systems which granted ALIVE several best research paper and presentation awards both local and abroad.

WEI-YUAN CHIANG received the B.S. degree in physics from Chung Yuan Christian University, Taoyuan, Taiwan, in 2001, and the M.S. and Ph.D. degrees in physics from the National Tsing Hua University, Hsinchu, Taiwan, in 2003 and 2008, respectively. He was an Assistant Professor at the Department of Electrical Engineering, Ming Chi University of Technology, Taiwan, from 2015 to 2020. He has been an Assistant Engineer with the Light Source Division, National Synchrotron Radiation Research Center, since 2021. His current research interests include electromagnetism, microwave source, microwave processing of advanced material, and microwave physics and engineering.